DETC 2003/DAC-48846

KINEMATICS OF WHEELED MOBILE ROBOTS WITH TOROIDAL WHEELS ON UNEVEN TERRAIN

Nilanjan Chakraborty
Robotics and CAD Laboratory
Department of Mechanical Engineering
Indian Institute of Science
Bangalore-560012
India.
Email: nchakraborty@mecheng.iisc.ernet.in

Ashitava Ghosal*
Robotics and CAD Laboratory
Department of Mechanical Engineering
Indian Institute of Science
Bangalore-560012.
India.
Email:asitava@mecheng.iisc.ernet.in

ABSTRACT

This paper deals with the kinematic analysis of a wheeled mobile robot (WMR) moving on uneven terrain. It is known in literature that a wheeled mobile robot, with a fixed length axle and wheels modeled as thin disk, will undergo slip when it negotiates an uneven terrain. To overcome slip, variable length axle (VLA) has been proposed in literature. In this paper, we model the wheels as a torus and propose the use of a passive joint allowing a lateral degree of freedom. Furthermore, we model the mobile robot, instantaneously, as a hybrid-parallel mechanism with the wheel-ground contact described by differential equations which take into account the geometry of the wheel, the ground and the non-holonomic constraints of no slip. Simulation results show that a three-wheeled WMR can negotiate uneven terrain without slipping. Our proposed approach presents an alternative to variable length axle approach.
Key Words: Wheeled vehicle kinematics, Uneven terrain, Slip-free motion.

INTRODUCTION

The motion of wheeled mobile robots (WMR) on flat terrain has been well studied due to its direct application in industrial environments (see for example, [1, 2]). More recently, mobile robots are being used in off-road navigation tasks and planetary exploration. The kinematic analysis proposed in [1, 2] cannot be applied directly to uneven terrain since on uneven terrain there can be slipping between the wheel-ground contact point. Waldron [3] has argued that two wheels independently joined to a common axle cannot roll on uneven terrain without slip. The use of Ackerman steering and differential wheel actuation which works for conventional vehicles on flat terrain does not work because there is no instantaneous center compatible with both wheels. Although a few WMR's capable of adapting to uneven terrain have been proposed in the literature [4–6] they are not capable of slip free motion. The lateral slip in WMR's is undesirable because it leads to *localization* errors thus increasing the burden on sensor based navigation algorithms. In addition, for planetary explorations, power is at a premium and such slipping leads to large wastage of power.

The problem of two wheels joined independently to a axle, moving on uneven terrain, without slip has been studied in [7–9]. In [9], the authors have modeled the vehicles as hybrid series parallel chains and using instantaneous rate kinematics showed that for prevention of slip, a) the line joining the wheel terrain contact points must be coplanar with the axle axis, or b) the wheels must be driven at identical speeds relative to the axle. In [8], the authors have suggested the use of a variable length axle (VLA) to overcome this problem, and they have proposed the use of an unactuated prismatic joint in the axle to vary the axle length. In [7], the instantaneous kinematics of a 3-wheeled vehicle with a VLA joining the two rear wheels have been studied. The authors have also provided experimental results regarding the variation of the

---

*Address all correspondence to this author.

length of the axle. In [5], the position kinematics of a wheeled actively articulated vehicle (WAAV) has been solved. This vehicle has the capability to adapt to uneven terrain but it is not capable of slip-free motion. A modification of the kinematic design of WAAV using VLA has been proposed in [10] and its kinematics has been studied. Vehicles with such a kinematic design to ensure no kinematic slipping has been termed as vehicles with slip-free motion capability (VSMC).

There are a few limitations of using a VLA – a) at high inclinations there is slipping due to gravity loading, and b) the dynamic slip due to inertial loading becomes large at higher speeds. To overcome the limitations in VLA, the use of an actuated VLA has been proposed. An actuated VLA, however, requires accurate measurement of slip to obtain the desired actuator output.

It may be noted that all the above mentioned work model the wheel as a thin disk. On a flat ground this is reasonable since the contact point always lies in a vertical plane passing through the center of the wheel. However on uneven terrain this is not the case in general and the contact point will vary along the lateral surface of the general wheel due to terrain geometry variations.

In this paper we have proposed an alternative to VLA for slip-free motion capability in wheeled mobile robots. Our alternative design is based on the following concepts:

- Each wheel is assumed to be a torus. The wheels and the ground are considered as rigid bodies and single point contact is assumed between the wheel and the ground. The equations describing the geometry of the wheel and the ground are assumed to be sufficiently smooth and continuous such that derivatives up to second-order exists and geometric properties such as curvature and torsion can be computed.
- The equations of contact between two arbitrary surfaces in single point contact, derived by Montana [11], are used to model the motion of a torus shaped wheel on an uneven terrain.
- The lateral rotational motion of the wheel is accommodated by a *passive* rotary joint. This allows the distance between the wheel-ground contact points to change without changing the axle length. Since this joint is passive, sensing or control is not required.
- *Instantaneously*, the wheeled mobile robot can be modeled as hybrid-parallel mechanism with a three-degree-of-freedom joint at the wheel-ground contact. Unlike a typical kinematic joint, the *no-slip* non-holonomic constraint leads to non-linear ordinary differential equations which are derived for the torus and smooth ground pair by following Montana [11].
- The position kinematics of the mobile robot is solved by integrating the ordinary differential equations and the holonomic constraints arising out of the hybrid-parallel mechanism. The set of differential-algebraic equations are solved

to obtain the position and orientation of the vehicle for given values of actuated variables and initial conditions.

We demonstrate our approach with a 3-wheeled vehicle and show by simulation that slip free motion can be achieved without a passive or actuated VLA. In our approach, no-slip motion is achieved by using torus shaped wheels and passive rotary joints without any additional sensors or control. This is the main contribution of this paper.

The paper is organized as follows: in the next section, we discuss the issues of modeling the uneven terrain. We assume that we have the terrain elevation data, from a sensor such as a laser range finder, at discrete points. These discrete points are interpolated using cubic splines which ensures sufficient smoothness and continuity. Subsequently, we state the contact equations derived by Montana and use them to derive the contact equations for a torus shaped wheel moving on uneven terrain. Then, we present our approach of modeling of the vehicle as a parallel manipulator instantaneously and derive the kinematic equations for it, followed by some simulation results, illustrating the capability of the vehicle to negotiate uneven terrain without slip. In the last section we present the conclusions and scope of future research.

MODELING OF UNEVEN TERRAIN

In this section, we review the differential-geometric properties of a surface required in our analysis and briefly present the concept of bi-cubic patch used to model the uneven terrain.

A surface in 3D space, $\Re^3$, can be expressed as a map of the form $\mathbf{X} : U \subseteq \Re^2 \to \Re^3$. In terms of coordinates, we have three equations, giving the (x, y, z) coordinates of a point on the surface as a function of two independent variables (u, v), of the form

$$(x, y, z)^T = \mathbf{X}(u, v)$$

At any point on the surface, we can define tangent vectors $\mathbf{X}_u$ and $\mathbf{X}_v$ as

$$\mathbf{X}_u = \frac{\partial \mathbf{X}}{\partial u} \qquad \mathbf{X}_v = \frac{\partial \mathbf{X}}{\partial v}$$

At any non-singular point, a normal to the surface can also be defined as

$$\mathbf{n} = \frac{\mathbf{X}_u \times \mathbf{X}_v}{|\mathbf{X}_u \times \mathbf{X}_v|}$$

We assume that $\mathbf{X}_u$ and $\mathbf{X}_v$ are orthogonal. This implies that the vectors $\{\frac{\mathbf{X}_u}{|\mathbf{X}_u|}, \frac{\mathbf{X}_v}{|\mathbf{X}_v|}, \mathbf{n}\}$ form a right-handed coordinate systems at any point on the surface. Based on this, we can define the following:

- A metric $[M]$ on the surface as

$$[M] = \begin{bmatrix} |\mathbf{X}_u| & 0 \\ 0 & |\mathbf{X}_v| \end{bmatrix}$$

- A curvature form $[K]$ as

$$[K] = \begin{bmatrix} -\mathbf{X}_{uu} \cdot \mathbf{n}/|\mathbf{X}_u| & -\mathbf{X}_{uv} \cdot \mathbf{n}/|\mathbf{X}_v| \\ -\mathbf{X}_{uv} \cdot \mathbf{n}/|\mathbf{X}_u| & -\mathbf{X}_{vv} \cdot \mathbf{n}/|\mathbf{X}_v| \end{bmatrix}$$

- A torsion form $[T]$ as

$$[T] = [\mathbf{X}_v \cdot \mathbf{X}_{uu}/|\mathbf{X}_u| \qquad \mathbf{X}_v \cdot \mathbf{X}_{uv}/|\mathbf{X}_v|]$$

We start with the assumption that we have the digital elevation model (DEM) of the terrain i.e., n available measured data points of the terrain in the form $(x,y,z)_i, \quad i = 1,2,...,n$. This data is assumed to be available from sensors located on the mobile robot or external to the robot. The reconstruction of a surface from its DEM is an ill-posed problem and a "correct" surface does not generally exist. As a result various notions such as least square error, distance metrics, energy minimization, smoothness assumptions on the underlying surface have been proposed in the literature to evaluate a reconstructed surface (for some of the techniques of surface reconstruction see, [12–14]). Each technique has its own strengths and drawbacks and finding an algorithm for efficient representation and accurate reconstruction of a surface is still an open problem. However, our focus in this paper is not on surface modeling techniques - in our analysis, we require a surface representation which enables us to compute up to second derivatives and any representation of the surface which allows us to do this will serve our purpose. Therefore, without loss of generality, in this paper we represent the surface as a simple bi-cubic patch.

A bi-cubic patch is given by the equation

$$\mathbf{X}(u,v) = \sum_{i=0}^{3}\sum_{j=0}^{3} a_{ij}u^i v^j \qquad (u,v)\varepsilon[0,1]$$

The quantities a_{ij}'s are called algebraic coefficients and there are 16 of them. One can find them from given 4 corner points and the slopes and twist vectors at these corner points. Alternatively, one can also find them if 16 points on the surface are given. The above equation of a bi-cubic patch can be differentiated twice and the required metric, curvature and torsion form can be computed efficiently. In a bi-cubic patch, a change in any of the algebraic coefficients(or any of the 16 points) changes the whole surface. For details see [15].

In this paper, we have used synthetic ground data for our simulation purposes. We have used in-built functions in Matlab [16] (Spline Tool Box) to generate a bi-cubic patch from given synthetic ground data and obtained the metric, curvature and torsion of the ground.

KINEMATIC MODELING OF SINGLE WHEEL

In this section, we derive the kinematic equations of contact of a torus shaped wheel rolling without slip on uneven terrain. For completeness, we present the differential equations describing contact between two smooth surfaces developed by Montana [11]. Then we use the same to find the contact equations for a single wheel moving on uneven terrain.

Figure 1 shows two surfaces 1 and 2 in contact with each other. The two surfaces are described relative to coordinate systems, $\mathbf{C_{r_1}}$ and $\mathbf{C_{r_2}}$, fixed to the two surfaces by $\mathbf{X_1} = \mathbf{X_1}(u_1, v_1)$ and $\mathbf{X_2} = \mathbf{X_2}(u_2, v_2)$ respectively. At the point of contact, coordinate systems $\mathbf{C_{l_1}}$ and $\mathbf{C_{l_2}}$ (which are fixed relative to $\mathbf{C_{r_1}}$ and $\mathbf{C_{r_2}}$) are defined on the two surfaces as follows:

- The coordinate system on surface 1 i.e. $\mathbf{C_{l_1}}$ is $\{\mathbf{X}_{u_1}/|\mathbf{X}_{u_1}|, \mathbf{X}_{v_1}/|\mathbf{X}_{v_1}|, \mathbf{n}(u_1, v_1)\}$
- The coordinate steam on surface 2 i.e. $\mathbf{C_{l_2}}$ is $\{\mathbf{X}_{u_2}/|\mathbf{X}_{u_2}|, \mathbf{X}_{v_2}/|\mathbf{X}_{v_2}|, \mathbf{n}(u_2, v_2)\}$

The four parameters (u_1, v_1), (u_2, v_2) (point of contact on surfaces 1 and 2 in $\mathbf{C_{r_1}}$ and $\mathbf{C_{r_2}}$ respectively) and the angle ψ between the X-axis of $\mathbf{C_{l_1}}$ and $\mathbf{C_{l_2}}$ are the five degrees of freedom between the two contacting surfaces. The angle ψ is chosen such that a rotation by angle $-\psi$ aligns the two X-axes. We can obtain the surface properties like metric $[M]$, curvature form $[K]$ and torsion form $[T]$ for both the surfaces using expressions provided in section 2. $[K^*]$, the curvature matrix of 2 at the point of contact relative to 1 is given by

$$[K^*] = [R_\psi][K_2][R_\psi]^T \qquad (1)$$

where $[R_\psi]$ is the matrix

$$[R_\psi] = \begin{pmatrix} \cos(\psi) & -\sin(\psi) \\ -\sin(\psi) & -\cos(\psi) \end{pmatrix}$$

The contact equations in the local frames $\mathbf{C_{l_1}}$ and $\mathbf{C_{l_2}}$ are given as [11]

$$(\dot{u}_1, \dot{v}_1)^T = [M_1]^{-1}([K_1] + [K^*])^{-1}[(-\omega_y, \omega_x)^T - [K^*](v_x, v_y)^T]$$
$$(\dot{u}_2, \dot{v}_2)^T = [M_2]^{-1}[R_\psi]([K_1] + [K^*])^{-1}[(-\omega_y, \omega_x)^T + [K_1](v_x, v_y)^T]$$
$$\dot{\psi} = \omega_z + [T_1][M_1](\dot{u}_1, \dot{v}_1)^T + [T_2][M_2](\dot{u}_2, \dot{v}_2)^T \qquad (2)$$
$$0 = v_z$$

3
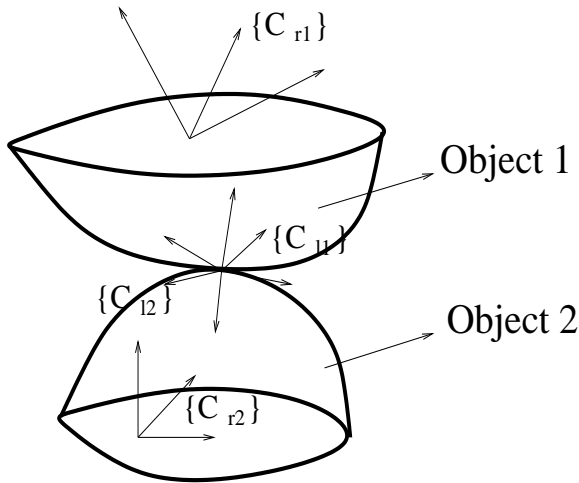
Figure 1.   TWO ARBITRARY SURFACES IN SINGLE POINT CONTACT.

Figure 2.   TORUS WHEEL ON UNEVEN TERRAIN.

where ω_x, ω_y and ω_z are the angular velocity and v_x, v_y and v_z are the linear velocity components of C_{l_1} relative to C_{l_2}. For rolling without slip v_x, v_y should be zero.

In our case surface 1 is the wheel (parametrized by (u_1, v_1)) and surface 2 is the ground (parametrized by (u_{g_1}, v_{g_1})). The geometrical properties of the ground, modeled as a bi-cubic patch, are determined as described in section 2. The wheel is modeled as a torus and its parametric equations in $\mathbf{C_{r_1}}$ is given by

$$x = r_1 \cos(u_1)$$
$$y = \cos(v_1)(r_2 + r_1 \sin(u_1)) \qquad (3)$$
$$z = \sin(v_1)(r_2 + r_1 \sin(u_1))$$

The wheel curvature, metric and torsion can be easily determined from the above equation.

In order to analyze the motion of the torus on the bi-cubic patch, we assign several coordinate frames. Figure 2 shows a torus wheel in a single point contact with the uneven ground. The frames $\{0\}$, $\{1\}$, $\{w\}$ and $\{2\}$ are frames $\mathbf{C_{r_2}}$, $\mathbf{C_{l_2}}$, $\mathbf{C_{r_1}}$ and $\mathbf{C_{l_1}}$ respectively. The transformation matrices to arrive at $\{w\}$ from $\{0\}$ as shown in figure 2 are given in Appendix A. We arrive at the contact equations of the torus shaped wheel rolling without slip on an arbitrary surface by putting v_x and v_y to zero in the equations(2). The simulation results of a single torus shaped wheel rolling without slip on uneven terrain is given in section 5.

KINEMATIC MODELING OF VEHICLE

We consider a 3-wheeled vehicle, designed for slip free motion, moving on uneven terrain. We consider two possible cases: vehicles with a top platform with three and six degree-of-freedom respectively.

3-DOF Vehicle

As mentioned earlier, we assume that the rear wheels have a degree-of-freedom at the wheel axle joint allowing lateral tilt. This allows the point of contact on the torus shaped wheel to vary along the u_1 coordinate during motion on uneven terrain. The front wheel can be steered and it has no lateral tilt capability. In this configuration, we can model the vehicle instantaneously as an equivalent hybrid-parallel mechanism as shown in figure 3.
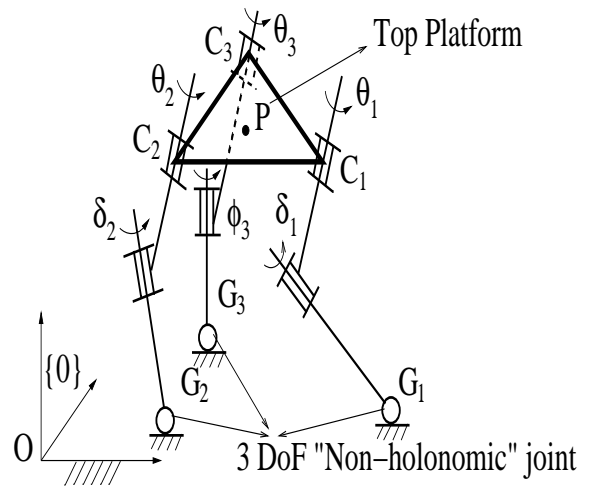
Figure 3.   EQUIVALENT INSTANTANEOUS MECHANISM FOR THE 3-DOF VEHICLE.

As mentioned in equation (2), at the wheel-ground contact point, we have one holonomic constraint, $v_z = 0$, which ensures contact is always maintained. Moreover, at each instant, we have 2 non-holonomic constraints which prevents instantaneous

4

sliding, and these are $v_x = 0$ and $v_y = 0$. Intuitively, this suggests us to model the wheel ground contact point, *instantaneously*, as a three-degree-of-freedom(DOF) joint. It may be noted that this joint is different from a three-DOF spherical joint due to the presence of 2 non-holonomic constraints which restrict the motion at any instant *only* in terms of achievable velocities[1]. In addition, the wheel-axle joints allowing rotation of the wheel, lateral tilt and steering respectively are modeled as 1 DOF rotary joints.

Now using Gruebler's criterion for a mechanism

$$DOF = 6(n - j - 1) + \sum f_i \qquad (4)$$

we find the DOF of the mechanism as 3, with total number of links n as 8, number of joints j as 9, and the total number of degrees of freedom (3 for each wheel ground contact and 1 for each of the 6 rotary joints), $\sum f_i = 15$. Therefore, three of the joint variables should be actuated and we choose rotation at the two rear wheels, θ_1 and θ_2, and the steering at the front wheel, ϕ_3, as the actuated variables. The two lateral tilts at the rear wheels, δ_1 and δ_2, and the rotation of the front wheel θ_3 are taken to be the passive variables which are to be computed.

6-DOF Vehicle
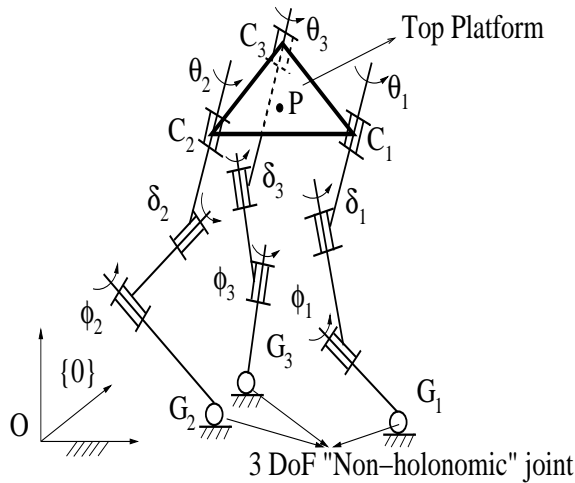
Figure 4. EQUIVALENT INSTANTANEOUS MECHANISM FOR THE 6-DOF VEHICLE.

In addition to the joints provided in the 3-DOF vehicle,

[1] As known in literature, non-holonomic constraints restrict only the space of achievable velocities and *not* the positions. A wheel or a thin disk undergoing rolling without slip, with $v_x = v_y = 0$, can reach any position in a plane and the only constraint is that of not leaving the plane and loosing contact

if we also provide a joint in each of the two rear wheels, to allow a steering degree-of-freedom in the wheels, and a joint in the front wheel to allow for lateral tilt in the front wheel, the instantaneous equivalent mechanism is as shown in figure 4. In this case $n = 11$, $j = 12$ and $\sum f_i = 18$. Therefore, using Gruebler's criterion we obtain the degrees of freedom of the top platform as 6, and would require 6 actuations to achieve the six degrees-of-freedom. In this paper, we present kinematic analysis and simulation results for a 3 DOF vehicle configuration. The analysis procedure, however, can be easily extended to a 6 DOF vehicle with actuated variables chosen as the rotation of the three wheels θ_1, θ_2, θ_3 and the three steering angles ϕ_1, ϕ_2, ϕ_3. The lateral tilt of the three wheels, δ_1, δ_2, δ_3, in this configuration would be the passive variables.

Kinematics of 3 DOF Vehicle

As the vehicle is subjected to non-holonomic no-slip constraints, the kinematics problem is formulated in terms of the first derivatives of the kinematic variables. The kinematic variables are obtained by integration since the no-slip constraints are non-integrable. The kinematics problem for the 3-DOF vehicle can be stated as follows:

Given the actuated variables, $\dot{\theta}_1$, $\dot{\theta}_2$, $\dot{\phi}_3$, and the geometrical properties of the ground and wheel, find $V_x, V_y, V_z, \Omega_x, \Omega_y, \Omega_z$, where V_x, V_y, V_z are the components of the linear velocity vector of the center of the platform (or any other point of interest) and $\Omega_x, \Omega_y, \Omega_z$ are the components of the angular velocity vector of the platform.

To solve this problem we proceed as follows:

- *Surface generation:*
  As described in section 2, we use 2-D cubic splines to reconstruct the surface from elevation data. From the interpolated surface we find expressions for the metric, curvature and torsion form for the ground. We also obtain expressions for the metric, curvature and torsion form for the torus shaped wheel.

- *Form contact equations:*
  For each wheel we write the 5 differential equations(see equation (2)) in the 15 contact variables u_i, v_i, u_{g_i}, v_{g_i}, and ψ_i, where $i = 1, 2, 3$. Since the wheels undergo no-slip motion, we set $v_x = v_y = 0$ for each of the wheels. It may be noted that ω_x, ω_y and ω_z in the contact equations for each wheel are the three components of angular velocities of frame $\{2\}$ with respect to frame $\{1\}$ and are unknown. These are related to the angular velocity of the platform $\Omega_x, \Omega_y, \Omega_z$ and the input and passive joint rates. In the fixed coordinate system, $\{0\}$, we can write

$$^0(\omega_x, \omega_y, \omega_z)^T = ^0(\Omega_x, \Omega_y, \Omega_z)^T - ^0\omega_{input} \qquad (5)$$

where $\omega_{input} = {}^0[\dot{R}]_{in}{}^0[R]_{in}{}^T$, and ${}^0[R]_{in}$ is given by ${}^0_w[R][R(e_3,\phi_i)][R(e_2,\delta_i)][R(e_1,\theta_i)]$ with $i = 1,2,3$, and $e_1 = (1,0,0)^T$, $e_2 = (0,1,0)^T$, $e_3 = (0,0,1)^T$. Appendix A gives the relevant transformation matrices for a wheel. Note that for the 3-DOF vehicle $\phi_1 = \phi_2 = \delta_3 = 0$.

The above equation (5) couples all 5 sets of ODE's and we get a set of 15 coupled ODE's in 21 variables. These are the 15 contact variables $u_i, v_i, u_{g_i}, v_{g_i}, \psi_i$ $(i = 1,2,3)$, the 3 wheel rotations $\theta_1, \theta_2, \theta_3$, the 2 lateral tilts δ_1, δ_2, and the front wheel steering ϕ_3. Out of these, the rates of the three actuated variables, θ_1, θ_2 and ϕ_3, are assumed to be known.

- *Form holonomic constraint equations:*
  In addition to the contact equations, for the 3 wheels to form a vehicle they must satisfy 3 holonomic constraint equations (refer to figure 3), namely

$$(\overrightarrow{OC_1} - \overrightarrow{OC_2})^2 = l_{12}{}^2; (\overrightarrow{OC_1} - \overrightarrow{OC_3})^2 = l_{13}{}^2; \qquad (6)$$
$$(\overrightarrow{OC_3} - \overrightarrow{OC_2})^2 = l_{32}{}^2;$$

  where $\overrightarrow{OC_1}$, $\overrightarrow{OC_2}$, $\overrightarrow{OC_3}$ are the position vectors of the center of the three wheels, C_1, C_2, C_3, respectively from the origin **O** of the fixed frame and l_{ij} is the distance between center of wheels i and j respectively.

- From the above steps, we have 15 first order ODE's and 3 algebraic constraint equations for the 18 unknown variables. This system of differential algebraic equations(DAE's) can be converted to 18 ODE's in 18 variables by differentiating the constraint equations and solved in any ODE solver with appropriate initial conditions. All the 18 ODE's mentioned above has been obtained using a symbolic manipulation package Mathematica [17].

- *Initial conditions:*
  To solve the set of 18 ODE's, we have to choose the initial conditions which satisfy both the holonomic constraint equations and the derivative of the constraint equations. Among the 18 variables we can choose $\delta_1 = 0, \delta_2 = 0, \phi_3 = 0$, initially. Moreover we can also choose v_1, v_2, v_3 to be $3\pi/2$ and the position of point of contact of any one wheel in $\{0\}$ (in our simulations, we have chosen the point of contact of wheel 2, given by u_{g_2}, v_{g_2}). The other two wheels must also be in contact with the ground. Hence, for each wheel, we have

$$\overrightarrow{OC_i} + {}^0_w[\mathbf{R}].\overrightarrow{C_iG_i} = \overrightarrow{OG_i}; \qquad i = 1,2,3 \qquad (7)$$

Converting them to unit vectors we have two independent

equations for each wheel. In addition, for each of the three wheels, we have,

$$\cos(\psi_i) = \hat{e}_{1_i}.\hat{e}'_{1_i} \qquad i = 1,2,3 \qquad (8)$$

where $\{\hat{e}_1, \hat{e}_2, \hat{e}_3\}$ and $\{\hat{e}'_1, \hat{e}'_2, \hat{e}'_3\}$ are the coordinate axes of reference frames $\{2\}$ and $\{1\}$ respectively in $\{0\}$ (refer to figure 2). In addition there are 3 holonomic constraint equations given by equation (6). This gives us 10 nonlinear equations in 10 variables and we can solve them numerically. It is to be noted that there can be more than one solution for the variables. However, we also have to check that the derivatives of the constraint equations are satisfied at the initial instant. We choose a solution set which satisfies the holonomic constraints and the derivative equations as our initial conditions.

- *Solve equations:* Using any ODE solver, solve the set of 18 ODE's, numerically with the initial conditions. Once we have obtained $u_i, v_i, u_{g_i}, v_{g_i}, \psi_i, i = 1,2,3$ and $\delta_1, \delta_2, \phi_3$ we can obtain the rotation matrix of the platform $[R_p]$. The position vector of the center of the platform $\overrightarrow{OP}$ with respect to the fixed frame, $\{0\}$, denoted by (x_c, y_c, z_c) is give by

$$(x_c, y_c, z_c)^T = \overrightarrow{OC_i} + [R_p]\overrightarrow{C_iP} \qquad (9)$$

for any $i = 1,2$ or 3 (see figure 3).

NUMERICAL SIMULATION AND RESULTS

In this section, we present numerical simulation results based on the equations developed in previous sections. We, first, present simulation results of a single wheel moving on uneven terrain without slip. Then we present three simulations of 3-DOF vehicle moving without slip on a flat terrain, piece-wise flat terrain and on an uneven terrain modeled as a bi-cubic patch.

Single wheel
The uneven terrain used for this simulation is shown in figure 5. As mentioned earlier, it was generated as a bi-cubic patch from synthetic digital elevation data. The metric, curvature and torsion form are obtained analytically for the torus shaped wheel and the uneven terrain. The set of 5 first order ODE's in $\dot{u}_1, \dot{v}_1, \dot{u}_2, \dot{v}_2, \dot{\psi}$ given in equation (2) are integrated using ODE45 in Matlab for a given $\omega_x, \omega_y, \omega_z$ (note $v_x, v_y = 0$ for no-slip and $v_z = 0$ to avoid loss of contact). For the simulation, the radii of the torus wheel are assumed to be $r_1 = 0.05m, r_2 = 0.25m$, and $\omega_x = 1, \omega_y = 0, \omega_z = 0.5$. The assumed initial conditions are $u_1 = \pi/2, v_1 = 3\pi/2, u_{g_1} = 0, v_{g_1} = 0, \psi = -\pi$. Figure 6 shows the variation of wheel parameters, u_1, v_1, and ψ. It can be seen

6

that the wheel tilts as it rolls on the uneven surface. Due to this, the trace of the wheel center and the contact point, as shown in figure 7, is different.
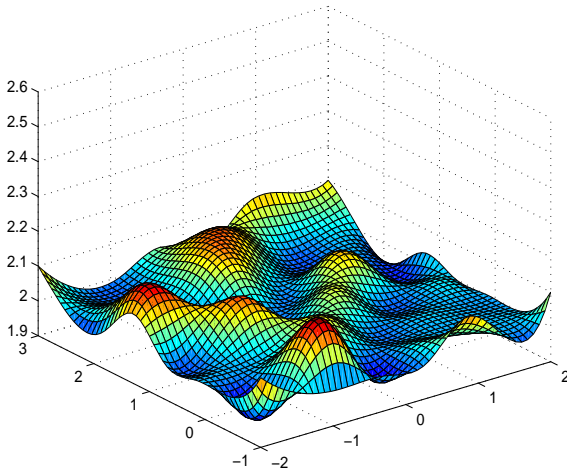
Figure 5. UNEVEN TERRAIN USED FOR SIMULATIONS.
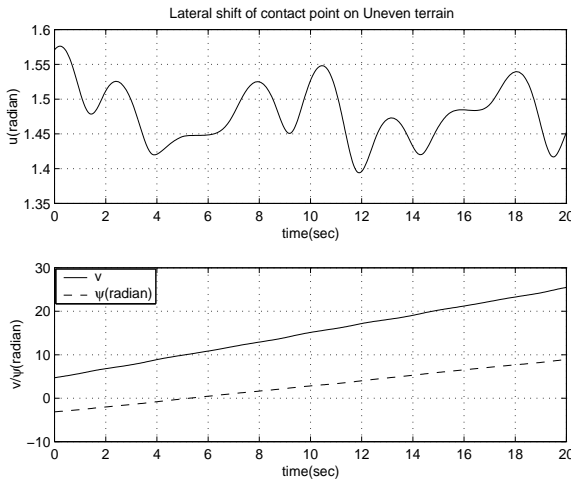
Figure 6. VARIATION OF PARAMETERS FOR SINGLE WHEEL MOVING ON UNEVEN TERRAIN.

3-DOF 3 wheeled vehicle
For the 3-DOF, three wheeled vehicle, analyzed in section 4, we use the following numerical values:

- Length of the rear axle $= 2l_a = 2m$.
- Distance of center of front wheel from middle of axle $= l_s = 1.5m$.
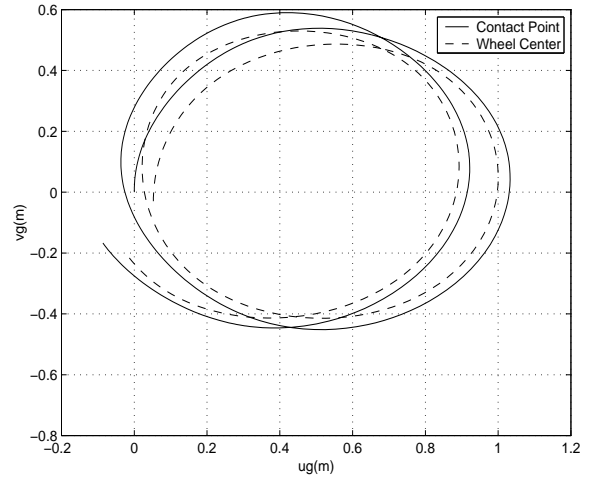
Figure 7. PLOT OF CENTER OF WHEEL AND GROUND CONTACT POINT FOR SINGLE WHEEL MOVING ON UNEVEN TERRAIN.

- Two radii of the torus shaped wheel are $r_1 = 0.05m, r_2 = 0.25m$.
- The center of the vehicle is assumed to be at $(1/3)l_s$ from the center of the axle along the line joining the center of the axle to the center of front wheel.

We present simulation results for the motion of the vehicle over three types of surfaces.

1. **Flat terrain:** The inputs and initial conditions used are $\dot{\theta}_1 = 0.7, \dot{\theta}_2 = 0.1, \delta_1 = 0, \delta_2 = 0$. On flat ground the vehicle has 2 DOF and ϕ_3, which remains constant, is given by

$$\tan\phi_3 = \frac{l_s(\dot{\theta}_1 - \dot{\theta}_2)}{l_a(\dot{\theta}_1 + \dot{\theta}_2)} \tag{10}$$

For simulation, the initial conditions chosen are:
$u_1 = \pi/2, v_1 = 3\pi/2, u_{g_1} = la, v_{g_1} = 0, \psi_1 = -\pi$
$u_2 = \pi/2, v_2 = 3\pi/2, u_{g_2} = -la, v_{g_2} = 0, \psi_2 = -\pi$
$u_3 = \pi/2, v_3 = 3\pi/2, u_{g_3} = 0, v_{g_3} = ls, \psi_3 = -\pi - \phi_3$

It can be seen, as expected, from figure 8 that there is no lateral tilt of the wheels when the vehicle is moving on flat ground. The holonomic constraints given by equation (6) are satisfied at all times as shown in figure 9. The locus of the center of the wheels, the wheel ground contact points and the center of the platform is shown in figure 10.

2. **Wheel 1 on an inclined plane and other two wheels on flat ground:** Figure 11 shows the 3-wheeled vehicle with one wheel on an inclined plane. The slope of the plane is taken to be 10°. The inputs and initial conditions used for the numerical simulation are as follows:

7

$\dot{\theta}_1 = 0.5, \dot{\theta}_2 = 0.4, \dot{\phi}_3 = 0.0005t, \delta_1 = 0, \delta_2 = 0, \phi_3 = 0$
$u_1 = \pi/2, v_1 = 3\pi/2, u_{g_1} = 1.04551, v_{g_1} = 0, \psi_1 = -\pi$
$u_2 = \pi/2, v_2 = 3\pi/2, u_{g_2} = -la, v_{g_2} = 0, \psi_2 = -\pi$
$u_3 = 1.57612, v_3 = 3\pi/2, u_{g_3} = 0.004635,$
$v_{g_3} = 1.49779, \psi_3 = -\pi$

To maintain no-slip motion and satisfaction of the holo-
nomic constraints, the torus shaped wheels must tilt in
the lateral direction. The variation of lateral tilts of the
rear wheels is shown in figure 12. The satisfaction of
holonomic constraints is depicted in figure 13, and the lo-
cus of the wheel center's, wheel-ground contact points and
the center of the three-wheeled vehicle is shown in figure 14.

3. **Bi-Cubic surface patch:** The bi-cubic surface patch used
is the same for the single wheel simulation and is shown
in figure 5. The inputs and initial conditions used for the
simulations are:

$\dot{\theta}_1 = 0.5, \dot{\theta}_2 = 0.4, \dot{\phi}_3 = 0, \delta_1 = 0, \delta_2 = 0, \phi_3 = 0$
$u_1 = 1.586967, v_1 = 3\pi/2, u_{g_1} = 0.983772, v_{g_1} = -0.037978,$
$\psi_1 = -3.140963, u_2 = 1.547598, v_2 = 3\pi/2, u_{g_2} = -la,$
$v_{g_2} = 0, \psi_2 = -3.144127, u_3 = 1.578296, v_3 = 3\pi/2,$
$u_{g_3} = 0.001578, v_{g_3} = 1.549151, \psi_3 = -3.143452$

The variation of lateral tilts of the rear wheels is shown
in figure 15. The satisfaction of holonomic constraints is
depicted in figure 16, and the locus of the wheel center's,
wheel-ground contact points and the center of the platform
is shown in figure 17.

In all the above cases, the no-slip conditions at the wheel
ground contacts are satisfied.
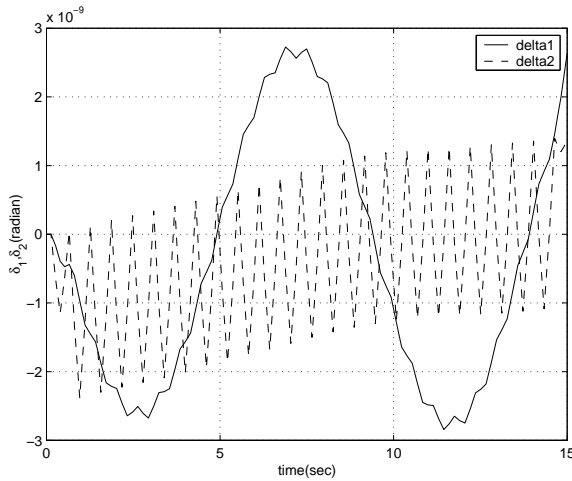
Figure 8. VARIATION OF LATERAL TILTS FOR 3-DOF VEHICLE MOV-
ING ON FLAT GROUND.
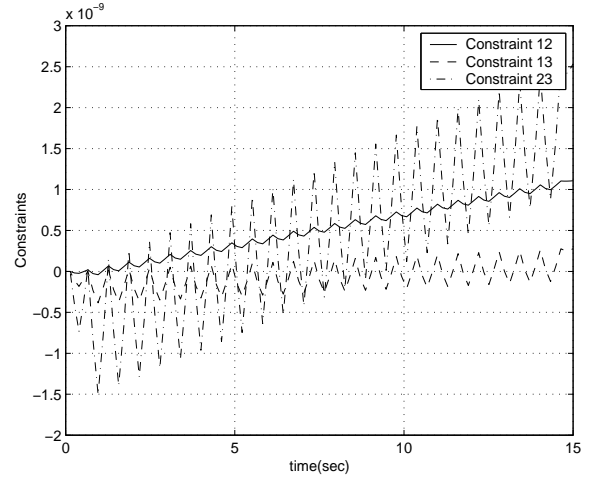
Figure 9. CONSTRAINT SATISFACTION FOR 3-DOF VEHICLE MOV-
ING ON FLAT GROUND.
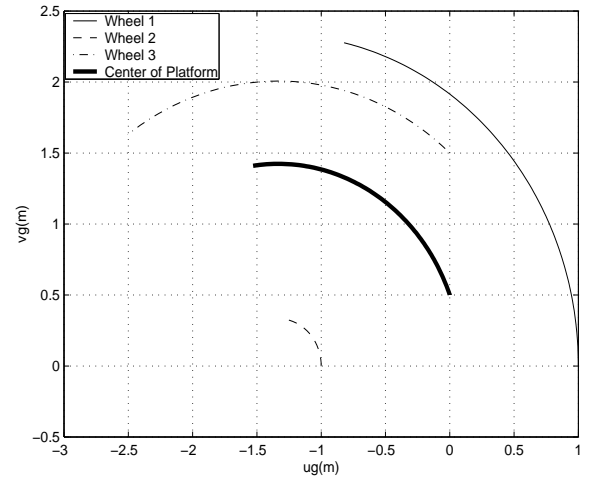
Figure 10. PLOT OF CENTER OF WHEELS AND PLATFORM FOR 3-
DOF VEHICLE MOVING ON FLAT GROUND.

CONCLUSION

In this paper we have studied the problem of kinematic slip
for mobile robots moving on uneven terrain. We have departed
from the conventional thin disk model and considered a torus
shaped wheel for motion with single point contact. This enables
us to take into account the lateral variation of the contact point
on the wheel when moving on uneven terrain. For eliminating
kinematic slip we have proposed the use of a joint which allows
lateral tilt of the wheels. We have demonstrated our approach

8
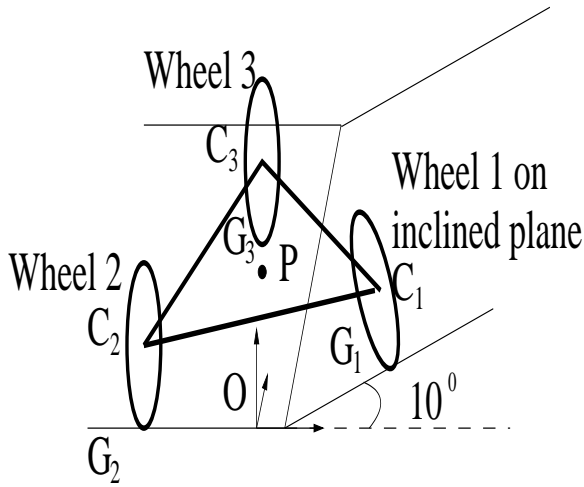
Figure 11. SCHEMATIC SKETCH OF 3-DOF VEHICLE WITH ONE WHEEL ON INCLINED PLANE.
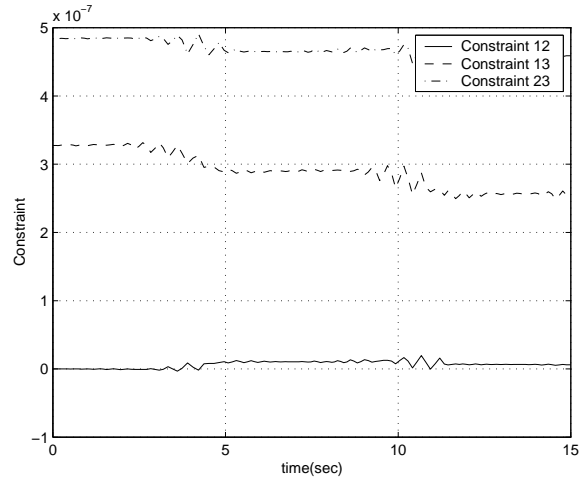
Figure 13. CONSTRAINT SATISFACTION FOR 3-DOF VEHICLE WITH ONE WHEEL ON INCLINED PLANE.
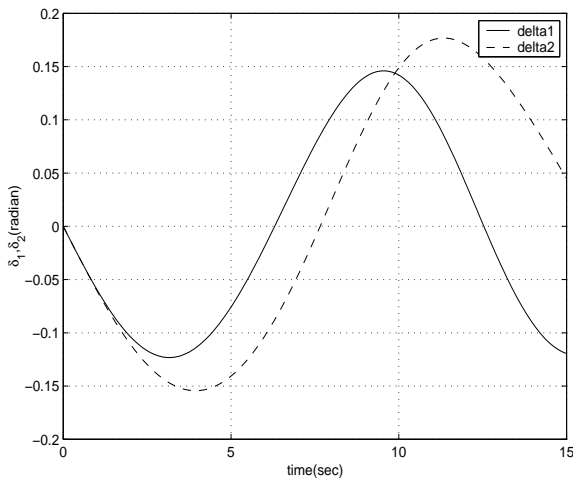
Figure 12. VARIATION OF LATERAL TILTS FOR 3-DOF VEHICLE WITH ONE WHEEL ON INCLINED PLANE.
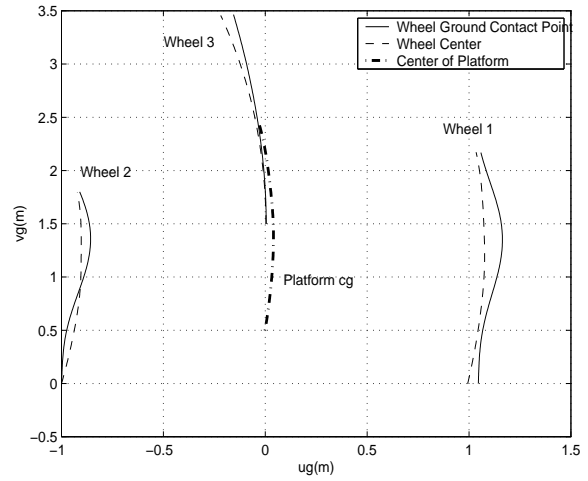
Figure 14. PLOT OF CENTER OF WHEELS, WHEEL GROUND CONTACT POINT AND PLATFORM CG FOR 3-DOF VEHICLE WITH ONE WHEEL ON INCLINED PLANE.

using a three wheeled vehicle, modeling the wheel-ground contact points as a 3-DOF joint with constraints described by ordinary differential equations. Numerical simulation results show that the vehicle modeled with torus shaped wheels and non-holonomic constraints at the wheel-ground contact, can negotiate uneven terrain without kinematic slip. This is an alternative to the variable length axle proposed in literature.

Our analysis is valid for any surface representation which provides up to second derivatives efficiently and accurately. Future work is being carried out on improved terrain modeling and representation. We are also investigating the ability of the vehicle to traverse uneven surfaces when joint limits are imposed on the lateral degrees of freedom. Finally, the dynamics of the vehicle on uneven surface is also being studied.

REFERENCES

[1] Alexander, J., and Maddocks, J., 1989. "On the kinematics of wheeled mobile robots". Int. Journal of Robotics Research, **8** (5) , pp. 15–27.

[2] Muir, P., and Neuman, C., 1987. "Kinematic modeling of wheeled mobile robots". Journal of Robotics Systems, **4** (2), pp. 281–329.
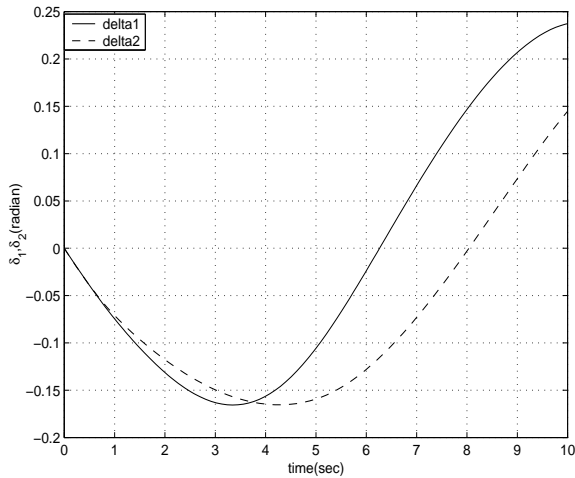
Figure 15. VARIATION OF LATERAL TILTS FOR 3-DOF VEHICLE MOVING ON UNEVEN TERRAIN.
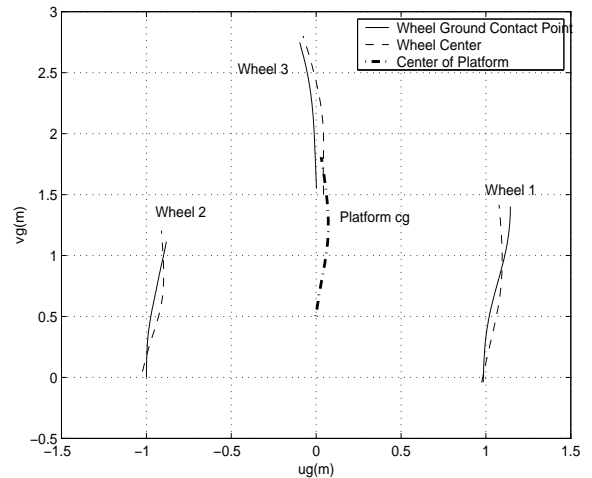
Figure 17. PLOT OF CENTER OF WHEELS, WHEEL GROUND CONTACT POINT AND PLATFORM CG FOR 3-DOF VEHICLE MOVING ON UNEVEN TERRAIN.
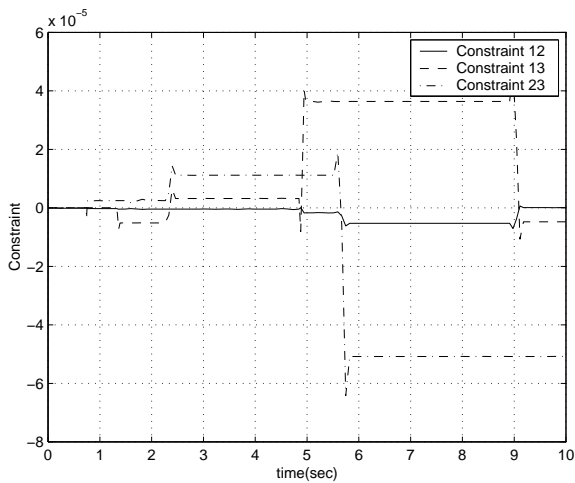
Figure 16. CONSTRAINT SATISFACTION FOR 3-DOF VEHICLE MOVING ON UNEVEN TERRAIN.

[3] Waldron, K., 1995. "Terrain adaptive vehicles". Trans. of ASME, Journal of Mechanical Design, **117B** , pp. 107–112.

[4] Bickler, D., 1998. "Roving over mars". Mech. Eng., **120** (4) , pp. 74–77.

[5] Sreenivasan, S., and Waldron, K., 1996. "Displacement analysis of an actively articulated wheeled vehicle configuration with extension to motion planning on uneven terrain". Trans. of ASME, Journal of Mechanical Design, **118** , pp. 312–317.

[6] Wilcox, B., and Gennery, D., 1987. "A mars rover for the 1990's". J. Brit. Interplanetary Soc.,[October].

[7] Choi, B., Sreenivasan, S., and Davis, P., 1999. "Two wheels connected by an unactuated variable length axle on uneven ground: Kinematic modeling and experiments". Trans. of ASME, Journal of Mechanical Design, **121** , pp. 235–240.

[8] Davis, P., Sreenivasan, S., and Choi, B., 1997. "Kinematics of two wheels joined by a variable-length axle on uneven terrain". In Proceedings ASME DETC'97. Paper no. DETC97/DAC-3857.

[9] Sreenivasan, S., and Nanua, P., 1996. "Kinematic geometry of wheeled vehicle systems". In Proceedings 24th ASME Mechanisms Conference. Paper no. 96-DETC-MECH-1137.

[10] Choi, B., and Sreenivasan, S., 1999. "Gross motion characterstics of articulated robots with pure rolling capability on smooth uneven surfaces". IEEE Trans. on Robotics and Automation, **15** (2) [April], pp. 340–343.

[11] Montana, D., 1988. "The kinematics of contact and grasp". Int. Journal of Robotics Research, **7** (3) , pp. 17–32.

[12] Amenti, N., Bern, M., and Kamvysselis, M., 1998. "A new voronoi-based surface reconstruction algorithm". In Proceedings SIGGRAPH '98, Addison Wesley Professional, pp. 415–421.

[13] Bajaj, C., Bernardini, F., and Xu, G., 1995. "Automatic reconstruction of surfaces and scalar fields from 3d scans". In Proceedings SIGGRAPH '95, Addison Wesley Professional, pp. 109–118.

[14] Edelsbrunner, H., and Mucke, E., 1994. "Three-dimensional alpha shapes". ACM Transactions on Graphics, **19** (1), pp. 43–72.

[15] Mortenson, M., 1985. *Geometric Modelling*. John Wiley and sons.

[16] 1992. *Matlab Users Manual*. MathWork Inc., USA.

[17] Wolfram, S., 1999. *The Mathematica Book*. Cambridge University Press.

Appendix A:

The transformation matrices for going from frame $\{0\}$ to frame $\{w\}$ are as follows:

$$
{}_1^0[\mathbf{T}] = \begin{pmatrix} l_1 & m_1 & n_1 & u_g \\ l_2 & m_2 & n_2 & v_g \\ l_3 & m_3 & n_3 & f(u_g, v_g) \\ 0 & 0 & 0 & 1 \end{pmatrix}
$$

where $l_i, m_i, n_i, i = 1, 2, 3$ are the components of the orthogonal vectors $\{\frac{\mathbf{f}_u}{|\mathbf{f}_u|}, \frac{\mathbf{f}_v}{|\mathbf{f}_v|}, \mathbf{n}\}$,$\mathbf{n}$ as defined in Section 2.

$$
{}_2^1[\mathbf{T}] = \begin{pmatrix} \cos\psi & -\sin\psi & 0 & 0 \\ -\sin\psi & -\cos\psi & 0 & 0 \\ 0 & 0 & -1 & 0 \\ 0 & 0 & 0 & 1 \end{pmatrix}
$$

$$
{}_3^2[\mathbf{T}] = \begin{pmatrix} \sin u & 0 & \cos u & 0 \\ 0 & 1 & 0 & 0 \\ -\cos u & 0 & \sin u & -r_1 \\ 0 & 0 & 0 & 1 \end{pmatrix}
$$

$$
{}_4^3[\mathbf{T}] = \begin{pmatrix} 1 & 0 & 0 & 0 \\ 0 & -\sin v & \cos v & 0 \\ 0 & -\cos v & \sin v & -r_2 \\ 0 & 0 & 0 & 1 \end{pmatrix}
$$

$$
{}_w^4[\mathbf{T}] = \begin{pmatrix} -1 & 0 & 0 & 0 \\ 0 & 1 & 0 & 0 \\ 0 & 0 & -1 & 0 \\ 0 & 0 & 0 & 1 \end{pmatrix}
$$